

Time correlation functions of hard sphere and soft sphere fluids

A. C. Brańka*

Institute of Molecular Physics, Polish Academy of Sciences, Smoluchowskiego 17, 60-179 Poznań, Poland

D. M. Heyes†

Chemistry Division, School of Biomedical and Molecular Sciences, University of Surrey, Guildford GU2 7XH, United Kingdom

(Received 29 September 2003; published 25 February 2004)

We explore the transition between soft particle fluids of increasing steepness to the hard sphere limit. We analyze the analytic forms of the time correlation functions used in determining transport coefficients in Green-Kubo formulas for fluids composed of particles interacting through a repulsive r^{-n} potential. We focus on the steeply repulsive $n \rightarrow \infty$ limit where the potential tends to the hard sphere interaction. Dufty [Mol. Phys. **100**, 2331 (2002)] developed a theoretical framework that can be used to characterize the transition from a steeply repulsive continuous potential toward the hard sphere potential for the shear stress time correlation function. This function was shown to consist of a rapidly decaying contribution (which is singular in the steeply repulsive limit) and a slowly decaying nonsingular part which can be reasonably well represented by Enskog's prediction on times of order and in excess of the mean collision time. We extend this treatment to the bulk viscosity and thermal conductivity. We focus on the bulk viscosity (pressure) correlation function as it is purely singular for hard spheres, and has no kinetic or cross term contributions in this limit. There is no relaxation of this correlation function on the mean collision or Enskog time scale for hard spheres. We show that it is *not* possible to represent the steeply repulsive behavior of this function *entirely* in terms of a sech function, i.e., $C_B(t) = \text{sech}(a_n t / \tau_n)$, where a_n is a numerical factor, t is time, and τ_n is a relaxation time proportional to n^{-1} . An additional singular function, which we call $w(t)$, is required to obtain the correct short-time behavior of $C_B(t)$ and the Enskog value for the bulk viscosity. With this additional function, the value of a_n in the $n \rightarrow \infty$ limit is $a_n = \sqrt{2}$ which is consistent with the second moment of the time expansion of the time correlation function. We compute this function for large n and extrapolate it to $n \rightarrow \infty$, determining one possible analytic form. The shear stress correlation function also gives $a_n = \sqrt{2}$ in the hard sphere limit for the singular part when the sech and w functions are used. This function has a nonsingular component, even in the hard sphere limit. We explore various forms for the crossover function $X(t/\tau_n)$ introduced by Dufty, which weights the limiting singular and nonsingular contributions to $C_S(t)$ particularly at intermediate times. The qualitative behavior for the heat flux time correlation function (used to obtain the thermal conductivity) is much the same as the shear case. The $w(t)$ derived by several self-consistent extrapolations appears, within the simulation statistics, to be the same for the bulk and shear viscosity, and for the thermal conductivity cases.

DOI: 10.1103/PhysRevE.69.021202

PACS number(s): 66.20.+d, 83.60.Bc, 66.60.+a

I. INTRODUCTION

The hard sphere fluid composed of particles interacting with the hard sphere potential,

$$\phi(r) = \begin{cases} \infty, & r \leq \sigma \\ 0, & r > \sigma, \end{cases} \quad (1)$$

has proved an invaluable reference fluid for the structural, thermodynamic, and dynamical properties of molecular and even colloidal liquids. Its popularity lies in its simplicity, which makes expressions for the structural and thermodynamic properties often more analytically tractable. The thermodynamic properties of the hard sphere system can be derived often with excellent accuracy at equilibrium fluid densities using the Carnahan-Starling equation of state [1],

$$\frac{P\beta}{\rho} \equiv Z = \frac{1 + \zeta + \zeta^2 - \zeta^3}{(1 - \zeta)^3}, \quad (2)$$

where P is the pressure of a pure hard sphere fluid or the osmotic pressure of a colloidal "hard sphere" liquid of such particles, $\rho = N/V$, the number density of N spheres in volume V ; and $\beta = 1/k_B T$ with k_B Boltzmann's constant and T the temperature. If $g(r)$ is the radial distribution function [2] then Z can be written in terms of its value at contact,

$$Z = 1 + \frac{2\pi\sigma^3\rho}{3} g(\sigma^+) = 1 + 4\zeta g(\sigma^+), \quad (3)$$

where $g(\sigma^+)$ is the value of $g(r)$ at contact, $r = \sigma^+$, where $\sigma^+ = \sigma + \delta$ for $\delta > 0$ and $\delta \rightarrow 0$. The packing fraction of hard spheres is $\zeta = \pi\rho\sigma^3/6$. Then from Eqs. (2) and (3) we have,

$$g(\sigma^+) = \frac{1 - \zeta/2}{(1 - \zeta)^3}, \quad (4)$$

*Electronic address: branka@ifmpan.poznan.pl

†Electronic address: d.heyes@surrey.ac.uk

For simplicity of notation we will replace σ^+ by σ henceforth.

However, we note that the hard sphere potential is discontinuous and nondifferentiable, and strictly speaking no real system can interact with a potential having this form. A consequence of the form of Eq. (1) is that the time correlation functions and hence the transport coefficients (using the Green-Kubo formulas [2]) are at least, in part, singular, as discussed recently by Dufty for the case of the shear viscosity [3]. Although the Green-Kubo (GK) formulas are often used to obtain transport coefficients from appropriate time correlation functions in molecular dynamics, the impulsive nature of the hard sphere potential and the resulting singularity in some of the time correlation functions causes the GK approach to be difficult to implement directly. Alder *et al.* [4] used a mean square displacement alternative to GK to obtain the shear and bulk viscosity, and thermal conductivity for hard spheres. This approach has been more recently discussed by Erpenbeck [5], and applied to continuous potential systems [6].

One can observe the onset of this singularity in a progressively systematic way by carrying out molecular dynamics simulations on a fluid with particles interacting via a continuous repulsive potential that can be forced to approach the hard sphere interaction by adjustment of one of its disposable parameters. For example, for a potential of the form

$$\phi(r) = \epsilon(\sigma/r)^n, \quad (5)$$

where ϵ and σ set the energy and length scales of the interparticle interaction, as $n \rightarrow \infty$ this potential tends to the hard sphere potential of Eq. (1). In a series of publications, some of the statistical mechanical foundations of the time correlation functions of this fluid in the steeply repulsive limit have been established [7–11]. The shear viscosity was considered first [7,8], and then the bulk viscosity [9]. This treatment was extended to the heat flux autocorrelation function $C_T(t)$ which gives the thermal conductivity in a Green-Kubo formula [10]. The main conclusion is that the effects of the “stiffness” (i.e., the value of n here) on the short-time part of the time correlation functions can be accounted for by a “renormalization” of the actual time by multiplication by the exponent n which measures the stiffness of the potential. We have shown that all of these many-particle correlation functions scale well according to nt up to times $nt \sim 1$ at least, and that they are, in part, singular at $t=0$ in the infinite n (the hard sphere) limit. Certain properties (such as the pressure and transport coefficients) are hardly distinguishable from those of hard spheres if the repulsion or stiffness parameter n exceeds about 72. While other properties such as the potential energy, infinite frequency elastic moduli, and the associated “viscoelastic” relaxations (as characterized by the time correlation functions) are highly stiffness dependent. Therefore, as the hard sphere limit is singular for some of these properties, it is important to establish how this limit is approached. We focus here on the time correlation functions used in the Green-Kubo formulas to calculate the transport coefficients.

II. THEORY

Consider a collective property transport coefficient χ representing either bulk or shear viscosity, or the thermal conductivity. The Green-Kubo formula for this quantity is

$$\chi = A \int_0^\infty \langle B(s+t)B(s) \rangle_s dt, \quad (6)$$

where $\langle \dots \rangle_s$ is a time correlation function averaged over a sampling time s which is also the simulation time in practice. The property B would be the shear stress for the shear viscosity, $P(t) - \langle P \rangle$ for the bulk viscosity [$P(t)$ is the instantaneous pressure and $\langle P \rangle$ is the average pressure], or the heat flux for the thermal conductivity. The constant A is a simple function of numerical prefactors and basic constants such as the volume of the system (V), the temperature T , and Boltzmann’s constant k_B . It is convenient to define a normalized time correlation function

$$C(t) = \langle B(s+t)B(s) \rangle_s / \langle B^2(s) \rangle_s, \quad (7)$$

which has the useful property in the present context that $C(0) = 1$. Substitution of Eq. (7) in Eq. (6) gives

$$\chi = C_\infty \int_0^\infty C(t) dt, \quad (8)$$

where

$$C_\infty = A \langle B^2 \rangle. \quad (9)$$

For the shear stress correlation function, $C_\infty \equiv G_\infty$ [9], the infinite frequency shear rigidity modulus, for the pressure correlation function, $C_\infty \equiv K_\infty - K_0$, the difference between the infinite frequency and zero frequency bulk moduli [9]. For the heat flux correlation function, $C_\infty \equiv M_\infty$, the so-called “thermal modulus” which was derived in Ref. [10]. Equation (8) gives $\chi = C_\infty \tau$ where $\tau = \int_0^\infty C(t) dt$ is a relaxation time, which is of the form proposed by Maxwell for the shear viscosity of gases [12]. For the collective quantity properties that we deal with here, $C(t)$ can be decomposed into a separate function derived entirely from the interaction potential, another which is purely kinetic, and another that is a mix of kinetic and interaction parts. We refer to these contributions to the correlation function, and the derived transport coefficient, as cc , kk , and kc .

In the steeply repulsive limit we follow Dufty [3] and separate the time correlation function $C(t)$ into a rapidly decaying part $C_1(t)$ which is a strong function of n and $C_2(t)$ which is more slowly decaying and relatively weakly sensitive to n , if at all. Dufty made an important contribution [3] in writing for the shear stress correlation function,

$$C(t) = C_1(t) + C_2(t) \approx \text{sech}(a_n t / \tau_n) + C_2(t). \quad (10)$$

$C_1(t)$ is singular because in the $n \rightarrow \infty$ limit, its unnormalized form diverges in height as a Dirac δ function. The non-singular part $C_2(t)$ is such that in the $n \rightarrow \infty$ limit and again unnormalized, it tends to a constant function. We already know from these previous studies that in the steeply repul-

sive limit the relaxation time τ_n for these functions is $\sim n^{-1}$ and $C_2(t)$ decays on the mean collision (Enskog relaxation) time, respectively, for the three transport coefficients [7–11]. The analytic form for $C_1(t)$ is not known exactly but a sech function has been shown to represent these correlation functions quite well [9,10] and has the necessary property in giving the exact second frequency moment of the expansion provided that $a_n = \sqrt{2}$. In the steeply repulsive limit we can replace $C_2(t)$ at long times by the Enskog prediction for any nonsingular part $C_E(t)$ divided by C_∞ . [Note that $C_2(0)$ is finite.] These requirements in the various limits suggest a plausible generic form for $C(t)$,

$$C(t) \approx \text{sech}(a_n t / \tau_n) + \frac{X(t/\tau_n)}{C_\infty} C_E(t), \quad (11)$$

where $X(x)$ is a ‘‘crossover’’ function with the properties that $X \rightarrow 0$ for $x \ll 1$ and $X \rightarrow 1$ for $x \gg 1$, and Dufty proposed

$$X(x) = \left(\frac{x^2}{1+x^2} \right)^2. \quad (12)$$

The C_∞ for the bulk and shear viscosity and thermal conductivity all diverge as ca. n in the steeply repulsive limit (see below). For the infinite frequency elastic shear modulus G_∞ [13],

$$G_\infty = \rho k_B T + \frac{2\pi\rho^2}{15} \int_0^\infty dr g(r) \frac{d}{dr} (r^4 \phi'), \quad (13)$$

where $\phi' \equiv d\phi/dr$. The infinite frequency shear modulus for this soft potential is obtained by substituting Eq. (5) in Eq. (13), giving the exact relation

$$G_\infty - \rho k_B T = \frac{1}{5}(n-3)(P - \rho k_B T), \quad (14)$$

where the pressure P is given by the virial expression

$$P - \rho k_B T = \frac{2\pi}{3} \rho^2 \int_0^\infty r^2 g(r) (-r \phi') dr. \quad (15)$$

In the large n limit we can write down an approximate yet accurate expression for G_∞ by ‘‘replacing’’ the real soft-core fluid by an equivalent hard sphere fluid with an effective hard sphere diameter σ_H [14]. In the steeply repulsive limit ($P - \rho k_B T$) in Eq. (14) can then be accurately approximated by that of hard spheres, ($P_H - \rho k_B T$), using the Carnahan-Starling hard sphere equation of state [1]. The result is

$$P_H - \rho k_B T = \frac{24}{\pi} \frac{k_B T}{\sigma_H^3} \zeta_H^2 \frac{(1 - \zeta_H/2)}{(1 - \zeta_H)^3}, \quad (16)$$

where $\zeta_H \equiv \pi N \sigma_H^3 / 6V$ is an effective hard sphere packing fraction. Substituting Eq. (16) in Eq. (14) gives

$$G_\infty - \rho k_B T \approx \frac{1}{5}(n-3) \frac{24}{\pi} \frac{k_B T}{\sigma_H^3} \zeta_H^2 \frac{(1 - \zeta_H/2)}{(1 - \zeta_H)^3}. \quad (17)$$

The bulk (‘‘compressional’’) modulus K_∞ [9] can be similarly obtained from

$$K_\infty - \frac{5}{3} \rho k_B T = \frac{2\pi\rho^2}{9} \int_0^\infty dr g(r) r^3 (r \phi'' - 2\phi'), \quad (18)$$

where $\phi'' \equiv d^2\phi/dr^2$, which for the inverse power potential gives the exact result

$$K_\infty - \frac{5}{3} \rho k_B T = \frac{1}{3}(n+3)(P - \rho k_B T), \quad (19)$$

which is approximately

$$K_\infty - \frac{5}{3} \rho k_B T \approx \frac{8}{\pi}(n+3) \frac{k_B T}{\sigma_H^3} \zeta_H^2 \frac{(1 - \zeta_H/2)}{(1 - \zeta_H)^3}. \quad (20)$$

In the steeply repulsive limit, $K_\infty \gg K_0$ so we can state that $K_\infty - K_0$ is approximately proportional to n in this case as well.

The heat conduction ‘‘modulus’’ M_∞ for the heat flux correlation function and thermal conductivity [10] can be obtained from

$$M_\infty - \frac{5}{2m} \rho k_B^2 T = \frac{k_B T}{m} \frac{\pi}{3} \frac{\partial}{\partial T} \left[\rho^2 \int_0^\infty dr g(r) r^4 \left(\phi'' + \frac{2}{r} \phi' \right) \right], \quad (21)$$

which for the inverse power potential gives

$$M_\infty - \frac{5}{2m} \rho k_B^2 T = \frac{1}{2}(n-1) \frac{k_B T}{m} \frac{\partial(P - \rho k_B T)}{\partial T}, \quad (22)$$

which is approximately

$$M_\infty - \frac{5}{2m} \rho k_B^2 T \approx \frac{12}{\pi m} (n-1) \frac{k_B^2 T}{\sigma_H^3} \zeta_H^2 \frac{(1 - \zeta_H/2)}{(1 - \zeta_H)^3}. \quad (23)$$

Therefore we note that M_∞ , G_∞ , and K_∞ are singular in the hard sphere (i.e., $n \rightarrow \infty$) limit. The formula proposed by Barker and Henderson for the effective hard sphere diameter σ_H , which is based on free energy arguments, was used in our previous publications [15]:

$$\sigma_H \equiv \int_0^\infty \{1 - \exp[-\beta\phi(r)]\} dr. \quad (24)$$

We can use Eq. (24) to define an effective hard sphere diameter and hence a corresponding packing fraction. Simulations carried out with various n values can then be carried out at the same effective hard sphere packing fraction [i.e., $\zeta_H \equiv (\pi/6)N\sigma_H^3/V$].

It can be seen from Eqs. (6), (7), and (11) that there is in general the possibility of singular and nonsingular contributions to the transport coefficients in the hard sphere limit. In the most general case, the transport coefficient has contributions from a purely kinetic part (‘‘ kk ’’), a purely collisional part (‘‘ cc ’’), and a cross term (‘‘ kc ’’) as discussed in Ref. [16]. We now consider each hard sphere transport coefficient and discuss the various contributions to the time correlation

function used in the Green-Kubo formula, indicating whether they are singular or nonsingular.

A. Shear viscosity

The unnormalized shear stress time correlation function of the hard sphere fluid consists of a singular term s , which is entirely cc in origin, and a nonsingular part u , which has the kk , kc , and the remainder of the cc part. The nonsingular part of the time correlation function $C_S^u(t)$ is [16]

$$C_S^u(t) = G'_\infty \exp(-t/\tau_S), \quad (25)$$

where

$$G'_\infty = \rho k_B T \left[1 + \frac{2}{5}(Z-1) \right]^2, \quad (26)$$

and $\tau_S = 5\sqrt{\pi}/24(Z-1)$ in hard sphere reduced units. The Enskog formula for the viscosity of the pure hard sphere fluid, η_s , is [16]

$$\eta_s/\eta_0 = \frac{\rho b}{Z-1} \left[\left(1 + \frac{2}{5}(Z-1) \right)^2 + \frac{48}{25\pi}(Z-1)^2 \right], \quad (27)$$

where $b = 2\pi\sigma^3/3$ is the second virial coefficient of the hard sphere fluid, Z is the compressibility factor defined in Eq. (2), and η_0 is the value of the shear viscosity in the limit of zero density. From kinetic theory,

$$\eta_0 = 1.016 \frac{5}{16\sigma^2} \left(\frac{mk_B T}{\pi} \right)^{1/2}, \quad (28)$$

which is independent of density. The first term in the square brackets in Eq. (27) is the nonsingular part (coming from the nonsingular part of the shear stress autocorrelation function) and the second term is the singular part. In other words the singular component of the viscosity η_s^s is

$$\eta_s^s/\eta_0 = \frac{32}{25} \rho \sigma^3 (Z-1). \quad (29)$$

The Green-Kubo integral of Eq. (25) yields the nonsingular part of the shear viscosity η_S^u ,

$$\eta_S^u/\eta_0 = \frac{\rho b}{Z-1} \left(1 + \frac{2}{5}(Z-1) \right)^2. \quad (30)$$

B. Thermal conductivity

The thermal conductivity follows the same trend as the shear viscosity. The nonsingular part of the heat flux relaxation function is

$$C_T^u(t) = M'_\infty \exp(-t/\tau_\lambda), \quad (31)$$

where

$$M'_\infty/k_B = \frac{5}{3} \rho k_B T \left[1 + \frac{3}{5}(Z-1) \right]^2, \quad (32)$$

and $\tau_\lambda = 5\sqrt{\pi}/16(Z-1)$ in hard sphere reduced units.

The Enskog formula for the thermal conductivity of the pure hard sphere fluid, λ , is [16]

$$\lambda/\lambda_0 = \frac{\rho b}{Z-1} \left[\left(1 + \frac{3}{5}(Z-1) \right)^2 + \frac{32}{25\pi}(Z-1)^2 \right], \quad (33)$$

where the value of the thermal conductivity in the limit of zero density, λ_0 , from kinetic theory, is given by

$$\lambda_0/k_B = 1.025 \frac{75}{64\sigma^2} \left(\frac{k_B T}{m\pi} \right)^{1/2}. \quad (34)$$

The singular component of the thermal conductivity λ^s is

$$\lambda^s/\lambda_0 = \frac{64}{75} \rho \sigma^3 (Z-1), \quad (35)$$

and the nonsingular part λ^u is

$$\lambda^u/\lambda_0 = \frac{\rho b}{Z-1} \left(1 + \frac{3}{5}(Z-1) \right)^2. \quad (36)$$

C. Bulk viscosity

The bulk viscosity of the hard sphere fluid is quite different from the previous two transport coefficients in only having a cc term and being entirely singular,

$$\eta_B/\eta_0 = \frac{32}{15} \rho \sigma^3 (Z-1), \quad (37)$$

where η_0 is defined in Eq. (28). The associated time correlation function $C_B(t)$ is singular which makes this function a ‘‘prototype’’ function and the most appropriate starting point to analyze the r^{-n} potential fluids in the steeply repulsive region.

D. Singular contribution

In the limit of $n \rightarrow \infty$ we have for the various infinite frequency moduli, from Eq. (17),

$$G_\infty(n) \rightarrow \rho k_B T \frac{n}{5} (Z-1), \quad (38)$$

from Eq. (20),

$$K_\infty(n) - K_0(n) \rightarrow K_\infty(n) \rightarrow \rho k_B T \frac{n}{3} (Z-1), \quad (39)$$

and from Eq. (23)

$$M_\infty(n) \rightarrow \rho k_B T \frac{k_B n}{2m} (Z-1). \quad (40)$$

We can assume that the singular part of the time correlation function $C^s(t)$ for each of the three transport coefficients is represented by $C^s(t) = \text{sech}(a_n t/\tau_n)$ where $\tau_n = \sigma_H(m/k_B T)^{1/2}/n$. A representation of the Dirac δ function is $\delta_n(t) = (a_n/\pi\tau_n) \text{sech}(a_n t/\tau_n)$ for $n \rightarrow \infty$ and $t > 0$. In the hard sphere limit a_n tends to a constant value, a say. Then, using the Green-Kubo formula,

$$\eta_S^s(n) \approx G_\infty(n) \frac{\pi \tau_n}{2a}, \quad (41)$$

$$\eta_B(n) \approx K_\infty(n) \frac{\pi \tau_n}{2a}, \quad (42)$$

and

$$\lambda^s(n) \approx M_\infty(n) \frac{\pi \tau_n}{2a} \quad (43)$$

in the hard sphere limit. Substitution of Eqs. (38)–(40) in Eqs. (41)–(43), respectively, gives analytic expressions for these transport coefficients in the hard sphere limit. These can be compared with the Enskog singular contributions to the transport coefficients, Eq. (29) for the shear viscosity, Eq. (37) for the bulk viscosity, and Eq. (35) for the thermal conductivity. Previous molecular dynamics (MD) simulations have shown that Enskog theory is essentially exact for all these transport coefficients up to a packing fraction of at least ca. 0.3 (see, e.g., Ref. [17]). In each case, agreement between the two expressions for each transport coefficient requires that $a = \pi^{3/2}/4$.

III. SIMULATION DETAILS

We have carried out molecular dynamics simulations on the inverse power potential fluids to explore the nature of the convergence of the time correlation functions for the r^{-n} fluids to the $n \rightarrow \infty$ hard sphere limit. Equilibrium MD simulations were carried out at $k_B T/\epsilon = 1$ on the potential of Eq. (5) with $n = 36$ –1152 in increasing multiples of 2 on $N = 500$ particle systems each for typically $(5-100) \times 10^6$ time steps ranging from 0.005 to $0.00008 \sigma(m/\epsilon)^{1/2}$ for $n = 36$ and 1152, respectively. The packing fractions $\zeta (= \pi N \sigma^3/6V)$ were chosen so that the computations were carried out at the same effective hard sphere packing fraction $\zeta_H = \pi \rho \sigma_H^3/6$ using the Barker-Henderson formula, Eq. (24), for these effective hard sphere diameters. Neighbor lists were implemented to reduce computer time, with an interaction cutoff r_c in each case based on the energy criterion $\phi(r_c) = \theta/\beta$ where $\theta = 10^{-4}$, which gives $r_c/\sigma = (\epsilon\beta/\theta)^{1/n}$. In presenting the results of these simulations, the unit of length is σ from Eq. (5), the unit of energy is ϵ from Eq. (5), and the unit of mass is the mass of the particle m . Therefore time t is in $\sigma\sqrt{m/\epsilon}$.

IV. RESULTS

In Fig. 1 we show the pressure (or “bulk”) normalized correlation functions $C_B(t)$ for a range of n plotted as nt and $\log(t)$ (inset). This figure shows that these correlation functions scale well as nt with increasing n , towards a limiting function. As discussed in Sec. II, the pressure correlation function is the most basic, as in the hard sphere limit it only has a cc component, which is also purely singular. For the range of n considered the kk and kc contributions to the pressure time correlation function and bulk viscosity are significantly smaller than the cc component, and so $C_B(t)$ is the

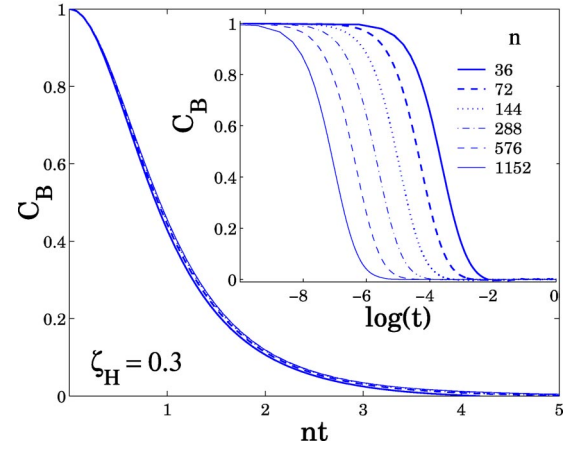


FIG. 1. The normalized bulk time correlation functions for steeply repulsive potential, SRP, vs nt for different n at the state point, $\zeta_H = 0.3$ and $T^* = 1$. In the inset the same functions are plotted vs $\log(t)$. [In this and subsequent figures, $\log(t) \equiv \log_e(t)$.] The unit of time, t , is $\sigma\sqrt{m/\epsilon}$ where σ and ϵ are taken from Eq. (5), and the unit of mass is the mass of the particle m .

most appropriate function to start our analysis. In Fig. 2 we show these normalized correlation functions plotted on a linear-log scale. This figure shows that at intermediate times the bulk correlation function decay is close to exponential, and converges to a limiting form in the steeply repulsive limit. We note that for ca. $nt > 3$ the data on the figure start to deviate from linearity [i.e., from an exponential form for $C_B(t)$]. There are several characteristics of this function. At short time it must decay as $1 - bt^2$, where b is a constant involving only basic quantities, as is necessary for all time correlation functions derived from continuous potentials [19]. It decays monotonically and in the intermediate time period, it has an exponential form, where nt time scaling is also evident. A functional form that satisfies these conditions is

$$C_B(t) \approx \text{sech}(a_n t / \tau_n), \quad (44)$$

where a_n is a parameter which is a function of n and temperature (and possibly density). In the previous papers in this

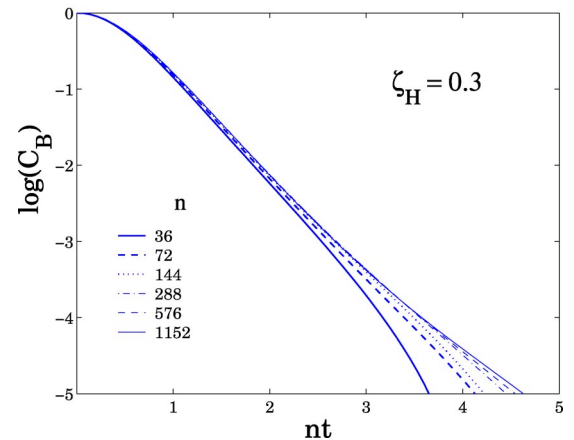


FIG. 2. Plot as Fig. 1 but $\log[C_B(t)]$ instead of $C_B(t)$ vs nt is plotted.

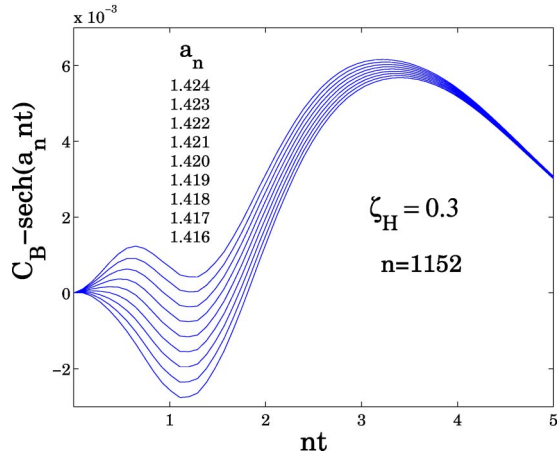


FIG. 3. The difference between $C_B(t)$ and $\text{sech}(a_n nt)$ vs nt for various values of the parameter a_n . The solid curves from top to bottom are for the decreasing a_n values, as given in the plot. The data are for $n = 1152$ and the effective hard sphere packing fraction $\zeta_H = 0.3$.

series [7–9,10,11], t/τ_n was written as $x = \sqrt{T^*} nt^*$ where $t^* \equiv (\epsilon/m\sigma^2)^{1/2} t$ and $T^* \equiv k_B T/\epsilon$. In this paper we will make the nt scaling more prominent by replacing x with nt since here we have $T^* = 1$ in all the simulation data presented. (In fact, the r^{-n} potential has the useful scaling feature that a computation carried out for $T^* \neq 1$ can be mapped onto a corresponding $T^* = 1$ state [18].) There is no a_n value, even for very large n , for which Eq. (44) applies at all times.

Figure 3 shows the difference between $C_B(t)$ and $\text{sech}(a_n nt)$ versus nt for a set of values of the parameter a_n . The solid curves from top to bottom are for decreasing a_n values, shown in the figure. The data are for $n = 1152$ and the effective hard sphere packing fraction $\zeta_H = 0.3$, although the trends are the same for other n and ζ_H values. The $\text{sech}(a_n nt)$ functional form has been proposed in the previous papers in this series for the short-time decay of the collective property time correlation function (see, e.g., Ref. [9]) but only with the specific value $a_n = \sqrt{2}$, the exact result based on a time expansion of the correlation function. To account for this deficiency, we express the bulk autocorrelation function of the r^{-n} fluids as the sum of two functions,

$$C_B(t) = \text{sech}(a_n nt) + w(a_n nt), \quad (45)$$

where the sech component is the dominant part and w can be considered as a perturbation or correction term. This additional term combined with the sech term gives us the necessary flexibility to satisfy the key requirements for $C_B(t)$. Although there are many possible “decompositions” of the $C_B(t)$ function, we consider Eq. (45) to be a reasonable match to the simulation data. The sech function is presumably not unique and so the analytic form of w will depend on the choice of the functional form of this main component of the singular part.

The form of the w function needs to be chosen using a reasonable criterion. We consider two possibilities. The first, which we refer to as method A, minimizes the integral of the function $w(a_n nt) = C_B(t) - \text{sech}(a_n nt)$. In practical terms,

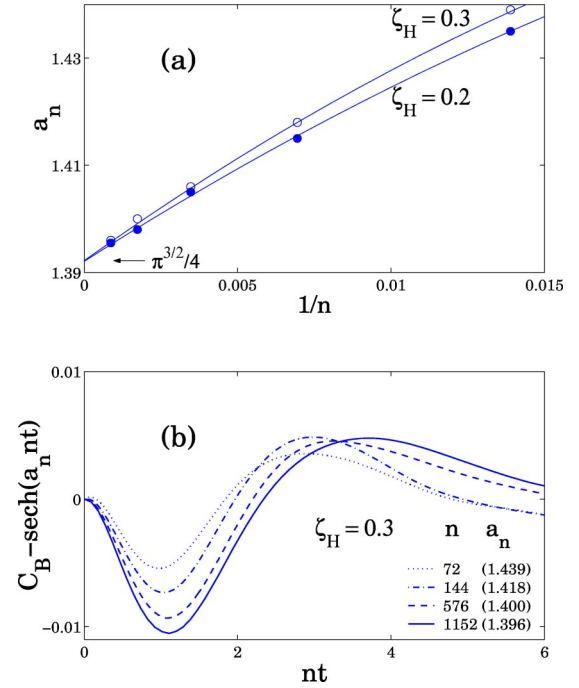


FIG. 4. (a) The upper graph shows the values of the parameter a_n vs $1/n$ estimated for different n from the condition that the time integral over the $w(t) = C_B(t) - \text{sech}(a_n nt)$ is zero (method A in the text). The open and closed circles represent the data for $\zeta_H = 0.3$ and $\zeta_H = 0.2$, respectively. The solid lines are second-order polynomial fits to the data and the arrow indicates a suggested value of a_n in the $n \rightarrow \infty$ limit. (b) The lower graph shows for $\zeta_H = 0.3$ and four different n values, the “perturbation” function $w(t) = C_B(t) - \text{sech}(a_n nt)$ using the a_n from the top figure.

we search for the value of a_n such that the integral of the w function tends to zero (typically the integral was < 0.0005). This criterion incidentally would allow us to obtain η_B directly from the sech function.

Figure 4(a) shows the values of the parameter a_n versus $1/n$ estimated for different n using the constraint that the integral over the $C_B(t) - \text{sech}(a_n nt)$ is zero. The open and closed circles represent the data for $\zeta_H = 0.3$ and $\zeta_H = 0.2$, respectively. The solid lines are second-order polynomial fits to the data and the arrow indicates a limiting (hard sphere) extrapolated value. Method A gives, within simulation uncertainty, the limiting value of $a_n \rightarrow \pi^{3/2}/4$ numerically for $n \rightarrow \infty$, which is Dufty’s prediction [3] for the shear stress time correlation function. If we follow Dufty’s approach for the pressure correlation function, by assuming that the singular part (here the only part) is represented by “sech,” then from the Green-Kubo formula we *must* have $a_n = \pi^{3/2}/4$ to give the Enskog value for the bulk viscosity, from Eq. (37), as discussed in Sec. II.

Figure 4(b) gives for $\zeta_H = 0.3$ and four different values of n , the “perturbation” function $w(t) = C_B(t) - \text{sech}(a_n nt)$, using the a_n values from the upper graph. In method A the integration should be performed in the time interval $t = 0 \rightarrow \infty$. In practice we have simulation data covering a finite time interval. The simulation data for $nt > 5$ were subject to increasing statistical uncertainty and so the upper time limit

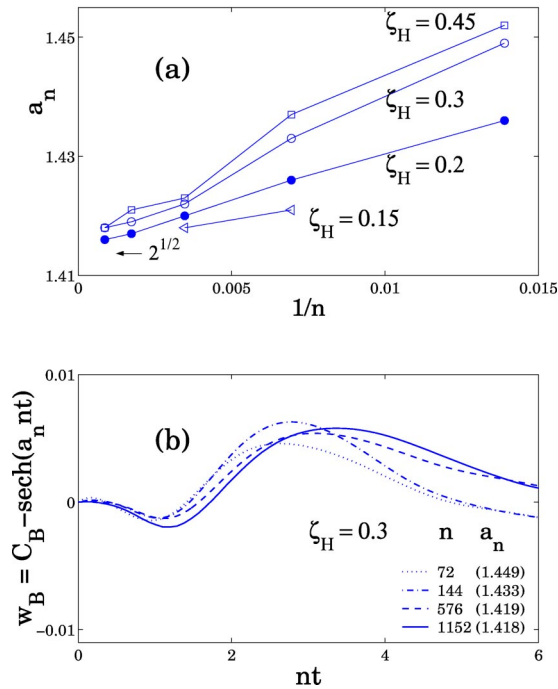


FIG. 5. Plot as for Fig. 4 but here the values of the a_n are estimated from the condition that the integral over $|C_B(t) - \text{sech}(a_n nt)|$ is a minimum (method *B* in the text). The data in the upper graph (a) are for four packing fractions. The solid lines drawn through the data for each packing fraction are to guide the eye and the arrow indicates the expected hard sphere limit. The lower graph (b) gives the “perturbation” function $w(t) = C_B(t) - \text{sech}(a_n nt)$ using the a_n from the top figure.

of the integral, t_u , had to be chosen carefully. The fitted solid lines changed only a little using upper values of $t_u = 5, 6, 7$, and 8. The data shown in Fig. 4(a) used a maximum nt value of 6 in the integral. The main conclusions are unaffected by the specific choice of the cutoff in the integral, in that the value of a_n with $1/n$ tends towards $\pi^{3/2}/4$ in the hard sphere limit, as expected from Dufty [3]. Also, the approximation of $\text{sech}(a_n nt)$ for C_B becomes less satisfactory with increasing n as rather large positive and negative deviations from zero in w are necessary to obtain a zero value for the integral [see Fig. 4(b)].

We explored another criterion, called method *B*, which was to minimize the integral of the absolute value of $|w(t)| = |C_B(t) - \text{sech}(a_n nt)|$. The advantage of this approach over method *A* is that we were more likely to get a better fit to actual form of $C_B(t)$, rather than just its integral which we have seen leads to quite large positive and negative values for the difference between $C_B(t)$ and $\text{sech}(a_n nt)$. Figure 5 shows the same quantities as given in Fig. 4 but with the values of a_n determined by this method. The data in the upper graph are for four packing fractions. The solid lines drawn through the data for each packing fraction are now just to guide the eye, and the arrow indicates the expected hard sphere limit based on a short-time expansion of the correlation function. Figure 5(b) shows the difference function $C_B(t) - \text{sech}(a_n nt)$ using the a_n from the top graph. Criterion *B* is better than *A* in that for short scaled times

(e.g., $nt < 2$), $C_B(t)$ is almost independent of n . Also for larger nt a more regular convergence trend to this limit is apparent. Figure 5(a) shows that method *B* gives a limiting value of a_n in the $n \rightarrow \infty$ limit that is statistically indistinguishable from $\sqrt{2}$, the exact result obtained from an expansion of the time correlation function [9]. Figure 5(b) also shows that the initial part of $w(t)$ is quite close to zero, which means that C_B can be very well represented (at least for small values of nt) by the sech function. Thus, the expansion $\text{sech}(a_n nt) = 1 - (a_n nt)^2/2 + O((nt)^4)$ can be fitted at short nt to the computed $C_B(t)$ to obtain a_n . We refer to this as the “parabolic” or “*D*” approach. We find that the *B* and *D* procedures both lead numerically to the correct value for a_n ($= \sqrt{2}$) in the hard sphere limit. They also give statistically the same dependence of a_n [and therefore $w(t)$] with $1/n$ and density, particularly for larger n (e.g., $n > 144$). For smaller n values there are differences between these two approaches which could be due to the finite value of the upper limit of nt in the integral and limitations in the numerical accuracy of the fitting procedure used in the *D* approach. Also the $w(t)$ function is not perfectly flat (i.e., zero) at short times (e.g., $nt < 0.1$). The parabolic approach has the advantage that it is simpler to implement and does not have the problem of establishing an upper time limit for the integral. As it leads to similar results to the w function of criterion *B* we have used the *D* method to obtain the a_n parameter for subsequent figures.

In Dufty’s method we only need the integral of $C_B(t)$ to give the Enskog result for the bulk viscosity and it is assumed that $C_B(t) = \text{sech}(a_n nt)$ which means that, as the integral C_B gives the Enskog value for the bulk viscosity, a_n must have the value $\pi^{3/2}/4$ (see Sec. II). This also emerges naturally from criterion *A* in which the integral of $w(t)$ is set to zero, so that as the integral of C_B is the integral of the sech function plus the integral of the w function, then we must have $a_n = \pi^{3/2}/4$ in this case also (as we found in Fig. 4). The limitation of the Dufty approximation is that the resulting short-time dependence of $C_B(t)$ is incorrect, as we require that $a_n = \sqrt{2}$ rather than $\pi^{3/2}/4$.

We found that the w data can be fitted well by the W function which is the sum of two Γ -distribution functions,

$$W(x) = W_1(x) + W_2(x), \quad (46)$$

where

$$W_1(x) = A_1 x^{a_1} \exp(-m_1 x^{k_1}), \quad (47)$$

and

$$W_2(x) = A_2 x^{a_2} \exp(-m_2 x^{k_2}). \quad (48)$$

We will use W_B to denote the W function for the case of the bulk viscosity time correlation function. $W_{B,n}$ is the analytic fit to w for a particular value of n . A fit to the simulation data using Eqs. (46)–(48) was made by minimizing the integral of $|W_{B,n}(t) - w_B(t)|$ until its value was $< 10^{-4}$. This gives eight parameters $A_1, a_1, m_1, k_1, A_2, a_2, m_2$, and k_2 of $W_{B,n}$. Figure 6 shows these fitted functions for the $n = 576$ and

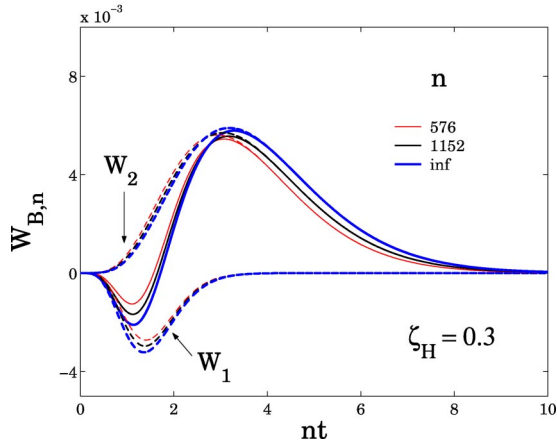


FIG. 6. A fit to the simulation data to Eqs. (46)–(48) by minimizing the integral of $|W_{B,n}(t) - w_B(t)|$ which yields the eight parameters $A_1, a_1, m_1, k_1, A_2, a_2, m_2$, and k_2 . On the scale of the figure the MD data are hardly distinguishable from the fits to at least $nt=5-6$. In the figure also the two components W_1 and W_2 are plotted as dashed lines. For the parameters, $A_1, a_1, m_1, k_1, A_2, a_2, m_2$, and k_2 in Eqs. (47) and (48), we have $-0.0244, 3.5864, 1.7852, 1.4890, 0.0045, 4.2378, 1.3888, 0.9738$ respectively for $n=576$, and $-0.0230, 3.7553, 1.9467, 1.3752, 0.0041, 4.4904, 1.5110, 0.9700$ for $n=1156$. Using the data for $n=576$ and 1152 and assuming linearity we calculated the limiting $W_{B,n}$ function in the $n \rightarrow \infty$ limit, which is given as the boldest solid line in the figure. This function has the parameters $-0.0221, 4.3447, 2.1588, 1.3383, 0.0036, 5.1865, 1.8565, 0.9380$, respectively.

1152 cases. On the scale of the figure the MD data practically lie on the fits for nt up to 5–6. The values for these eight constants in each case are given in the figure caption. $W_1(x)$ are the dashed lines with the minimum, and $W_2(x)$ are the dashed lines with the maximum. We see from the simulation data shown in Fig. 5 that at least for large n it is reasonable to assume that a linear expansion in $1/n$ can be used to extrapolate $W_{B,n}(t)$ to the limit $n \rightarrow \infty$ limit [i.e., to give $W_{B,\infty}(t)$]. Using the data for $n=576$ and 1152 and assuming this linearity, the limiting $W_{B,n}$ function was obtained and is shown as the boldest line in Fig. 6. These fit parameters are also given in the figure caption.

In the limit $n \rightarrow \infty$ the constant $a_n = \sqrt{2}$ (see Fig. 5) and $C_B(t)$ therefore tends to $\text{sech}(\sqrt{2}nt) + W_{B,\infty}(nt)$. We know from Enskog theory the value of the integral of C_B , and we can calculate the integral of the sech function to determine the integral of the perturbation term w_B . The integral of $W_{B,\infty}$ which we call W_I has the value $(2\sqrt{2}/\pi - \pi/2)/\sqrt{2} \approx 0.0177$. Thus, we have an additional condition that allows us to check (and justify) our linear extrapolation in $1/n$. As $\int_0^\infty [x^a \exp(-mx^k)] dx = \Gamma((a+1)/k)/k/m^{(a+1)/k}$ then,

$$W_I = \int_0^\infty W_{B,\infty} dx = A_1 \Gamma((a_1+1)/k_1)/k_1/m_1^{(a_1+1)/k_1} + A_2 \Gamma((a_2+1)/k_2)/k_2/m_2^{(a_2+1)/k_2} = 0.0176, \quad (49)$$

using the parameters given in the caption to Fig. 6, and which is very close to the exact value $W_I = 0.0177$. As our

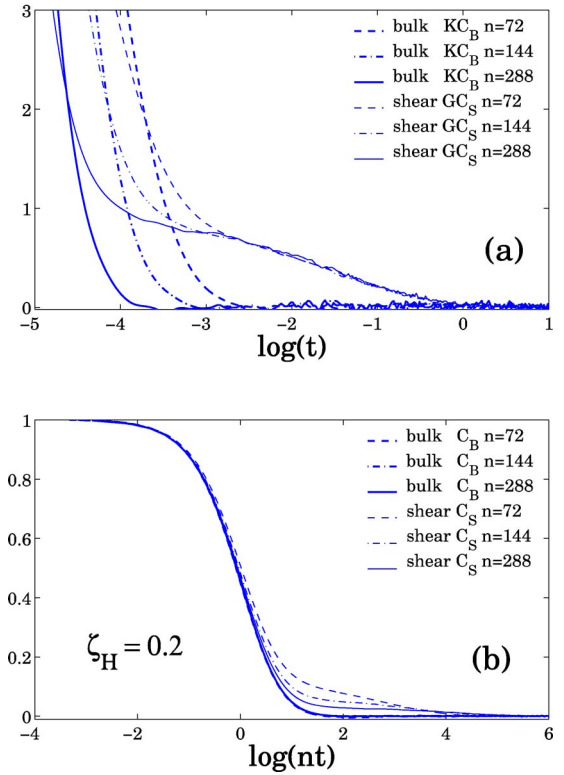


FIG. 7. The bulk and shear time correlation function for r^{-n} fluids with $n=72, 144$, and 288 at $\zeta_H=0.2$. The upper graph (a) shows these functions vs $\log(t)$. In the lower graph (b) the same data are shown as functions normalized to unity at zero time, and now plotted vs $\log(nt)$.

simulation data become statistically more unreliable in the range $5 < nt < 6$, it is difficult to make any firm statements about the analytic form of any limiting “tail” in the w_B function. Of course, any tail present in w_B need not have the $\exp(-m_2 x^k)$ analytic form. Figure 6 also shows that for $nt > 4$ we have $w_B \approx W_2$. A plot of the w_B function on a linear-log scale shows a near linear behavior for $nt > 4$. One can also observe that k_2 is close to 1 (in fact calculations performed with $k_2=1$ fixed gave a fit that was almost as good as when k_2 was a free variable). Thus, an exponential decay of the form $\exp(-m_2 x)$ at long times is quite possible. The value of $W_I = 0.0176$ for the particular set of data a_n for $n=576$ and 1152 at $\zeta_H=0.3$ is very close to the exact value 0.0177 . For the $\zeta_H=0.2$ data, a value of 0.0162 was obtained. Nevertheless, the limiting function was always very close to that in Fig. 6, and the deviations from the exact value of 0.0177 we think are mainly produced by the less accurate tail data for $nt > 4$. We would add that, of course, the fitting procedure is not unique, and other analytical forms for the $W_{B,n}$ functions are possible (perhaps with fewer free parameters) and so we assume that the coefficients A_1, \dots, k_2 have no physical meaning.

We now consider the shear stress correlation function $C_S(t)$. The unnormalized bulk and shear time correlation functions for various values of n are given in Fig. 7. The upper figure (a) shows the functions versus $\log(t)$ for the packing fraction $\zeta_H=0.2$. We denote the quantity C_∞ [see

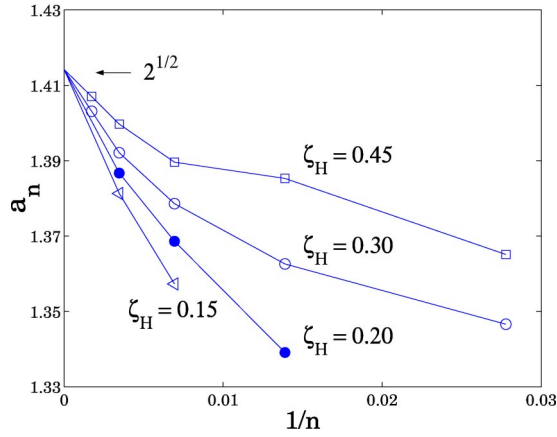


FIG. 8. The parameter a_n vs $1/n$ estimated from the short-time expansion or D approach applied to the $C_S(t)$. The solid lines drawn through the data for each packing fraction are to guide the eye and the arrow indicates the analytically exact result [9].

Eq. (9)] by K and G for the bulk and shear functions, respectively. The lower figure shows the same data, but normalized so that $C_B(0) = C_S(0) = 1$, and now plotted versus $\log(nt)$. This form of plotting emphasizes the singular part of the decay in the correlation function. Notice in Fig. 7(a) the gradual appearance of a shoulder in $C_S(t)$ at intermediate times with increasing n , which is most prominent in the $n = 288$ data of the figure. The soft system with increasing potential stiffness (i.e., n) is tending to the hard sphere fluid. The nonsingular part of the decay should follow closely the Enskog formula for the hard sphere shear stress correlation function, given in Eq. (25). Figure 7(b) illustrates that the behavior of the singular part of C_S is very similar to that of the C_B . Thus, it is reasonable to assume that the singular part of the C_S can be well represented by the $\text{sech}(a_n nt)$ function, as proposed by Dufty. The parameter a_n can be determined from the short-time part of C_S as for C_B , using the D approach for example. This is a key point as it allows us to subtract off the (main) singular part. At long times and for large n we expect $C_S(nt) - \text{sech}(a_n nt)$ to be quite close to the nonsingular part as given by Enskog theory [Eq. (25)] divided by G_∞ . In Fig. 8 we show the parameter a_n versus $1/n$ estimated from the short-time D expansion approach. In the hard sphere limit we see that $a_n \rightarrow \sqrt{2}$, the analytically correct result [9]. Figure 9 focuses on the part of the stress relaxation that is dominated by the nonsingular component. The figure shows the normalized shear stress time correlation function, after subtraction of the main singular part, compared with the Enskog prediction. For each n the corresponding value of a_n from Fig. 8 was used in the sech subtraction procedure. The dashed line represents the Enskog function divided by the shear modulus G_∞ , which is seen to follow the simulation data very well.

From our treatment of the C_B data we know that the singular part is not exactly represented by the $\text{sech}(a_n nt)$ function, but requires an additional term $w(t)$. To distinguish the $w(t)$ functions in the bulk and shear cases, we refer to them as w_B and w_S , respectively. Therefore we think that the shear function is not best represented by Eq. (11) but by the more general formulation,

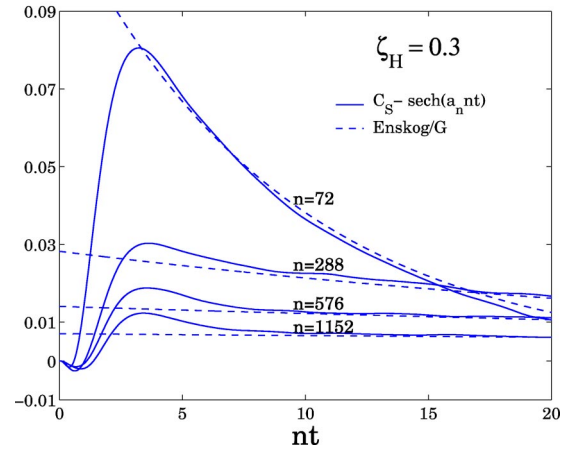


FIG. 9. The normalized shear stress time correlation function after subtraction of the main singular part vs nt (solid line). For each n , the a_n value shown in Fig. 8 was applied. The dashed line represents the Enskog function divided by the shear modulus G ($\equiv G_\infty$).

$$C_S(t) = \text{sech}(a_n nt) + w_{S,n}(t) + \frac{X(nt)}{C_\infty} C_{S,E}(t). \quad (50)$$

The X function in Eq. (50) controls the crossover from the time scale characterizing the collision to the Enskog time scale, which is of order the mean time between collisions. We now have two unknown functions $w_{S,n}(t)$ and $X(nt)$, which require additional information or assumptions, as we cannot separate C_S in a unique way into these two components. We can assume a general form for the X function, with a single disposable parameter function. We can impose the condition that the limit of the integral over $w(t)$ has to go linearly (in n^{-1}) towards the Enskog (HS) limit. Dufty proposed a number of requirements for $X(t)$ that it must be even in time, vanish up through order $\sim t^2$, and approach unity at long times. Even if we assume the same general form for the w_S function as for w_B , (i.e., two Γ distribution functions) we still have to choose an analytic form for the X function. Apart from the general conditions given by Dufty, we can require that the limiting form of the singular part of the shear correlation function should be the same as that of the bulk auto-correlation function. In the limit $n \rightarrow \infty$, we must have $a_n \rightarrow \sqrt{2}$ for both functions. For large n the $w_S(n)$ functions are expected to converge linearly in $1/n$ towards the $W_{S,\infty} = W_{B,\infty}$ limit, which we now know reasonably well in the bulk case. Therefore the time integral of w_S should be 0.0177, and an acceptable analytical form for the X function is one that gives this limiting behavior. This assumption then allows us to say something more about the X function. Three plausible choices for the X function are $X_1(x) = x^2/(A + x^2)$, where A is a parameter, $X_2(x) = [x^2/(1 + x^2)]^2$, which is Dufty's proposal of Eq. (12), and

$$X_3(x) = [x^2/(A + x^2)]^2, \quad (51)$$

which is a generalization of Dufty's function with one disposable parameter. Therefore we have, in the latter case,

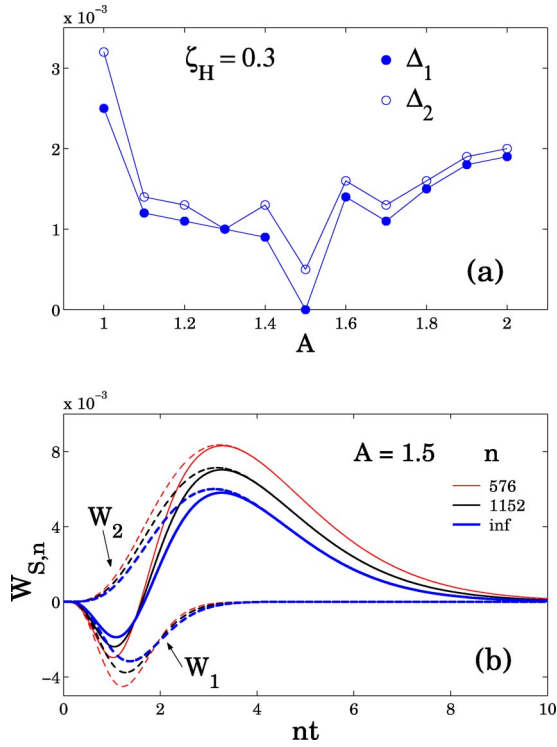


FIG. 10. The top figure shows $\Delta_1 = \int dt W_{S,\infty}(t) - 0.0177$ and $\Delta_2 = \int dt |W_{S,\infty}(t) - W_{B,\infty}(t)|$ plotted as a function of the A parameter given in Eq. (51). $W_{S,\infty}$ was obtained from linear extrapolation of $W_{S,576}$ and $W_{S,1152}$ together with the X_3 crossover function given in Eq. (51). In (b) the results for $W_{S,n}$ obtained with the X_3 are shown (this is analogous to Fig. 6).

$$w_{S,n}(t) = C_S(t) - \text{sech}(a_n nt) - X_3(nt) C_{S,E}(t)/G_\infty, \quad (52)$$

where $C_{S,E}(t)$ is given in Eq. (25). For convenience we define

$$\Delta(t) = X_3(nt) C_{S,E}(t)/G_\infty. \quad (53)$$

The quantities $\Delta_1 = \int_0^\infty dt W_{S,\infty}(t) - 0.0177$ and $\Delta_2 = \int dt |W_{S,\infty}(t) - W_{B,\infty}(t)|$ are plotted in Fig. 10(a) as a function of the parameter A . $W_{S,\infty}$ was obtained from linear extrapolation in n^{-1} of $W_{S,576}(t)$ and $W_{S,1152}(t)$ determined in conjunction with the X_3 function. The calculations are for 11 values of the parameter A . The same form of the fitting function was used as in the case of the bulk w_B function, i.e., Eqs. (46)–(48). There are minima in these two difference functions in the range $1.4 < A < 1.6$, which indicates that the particular function $X_3(x) = [x^2/(1.5+x^2)]^2$ satisfies these limiting conditions very well. The performance of X_2 and X_1 (with $1 < A < 2$) was not as good. In Fig. 10(b) the results for $W_{S,n}$ obtained with $X_3(x) = [x^2/(1.5+x^2)]^2$ are shown (this is analogous to Fig. 6).

The assumption that, in the limit $n \rightarrow \infty$, the singular parts of C_S are the same as that of C_B is open to debate. Exactly in the limit $n = \infty$ (i.e., hard sphere limit) we have a δ function for the singular part, which has many possible representations, not just the sech form. Even for finite n there are many possible representations consistent with the simulation data.

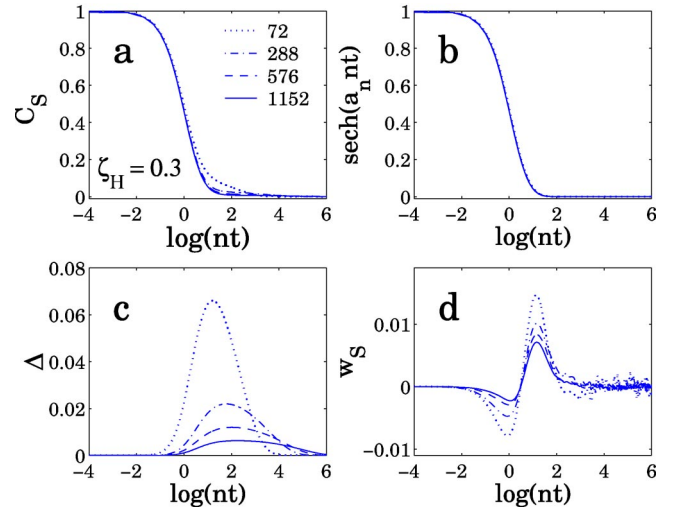


FIG. 11. Decomposition of the shear time correlation function into singular and nonsingular components, all vs $\log(nt)$ is shown for each value of n . Key: (a) The normalized $C_S(t)$ function with $n = 72, 288, 576$, and 1152 for the packing fraction $\zeta_H = 0.3$. (b) The main or singular part, $\text{sech}(a_n nt)$. (c) The nonsingular or Enskog-limiting part, defined in Eq. (53), $\Delta(t)$. (d) The “perturbation” singular part $w_S(t)$ defined in Eq. (52). In the calculations a_n taken from Fig. 8 are used. The X_3 function with $A = 1.5$ was used.

In contrast, the X function could have a physical basis, with a unique functional form, as it weights the singular and Enskog contributions as a function of time. Thus, the X_3 analytic form, with the value $A = 1.5$, might not only be a useful empirical function to describe C_S , but indicate something more fundamental. As for the bulk time correlation function we also obtain the integral of $W_{S,\infty} = 0.0177$, which is the exact value [see the black dot for Δ_1 in Fig. 10(a) at $A = 1.5$].

The results of our decomposition of $C_S(t)$ are presented for the shear case in Fig. 11 using data taken from simulations carried out at a packing fraction of $\zeta_H = 0.3$. This figure shows the various components of the shear time correlation function versus $\log(nt)$ for four values of n , ranging from 72 to 1152. Figure 11(a) gives the “total” normalized C_S function, which illustrates the very good nt scaling, at least at short times (nt). Figure 11(b) shows the main or singular part, $\text{sech}(a_n nt)$, with the a_n values given in Fig. 8. It can be seen that the four curves are essentially indistinguishable on this scale. In Fig. 11(c) the nonsingular or Enskog-like part, $\Delta(t)$, defined in Eq. (53), is shown for the four data sets. In Fig. 11(d) the perturbation singular part $w_S(t)$ defined in Eq. (52) is shown for each value of n [see Fig. 11(a) for the key]. The $w(t)$ functions in the hard sphere limit for the shear and bulk cases are statistically indistinguishable, as seen in Fig. 12 and we might therefore expect that both shear and bulk $w(t)$ converge to the same functional form.

The trends for the heat flux time correlation functions C_T are similar to the C_S . Figure 13 shows the unnormalized C_T versus $\log_e(t)$ for different n values at the packing fraction $\zeta_H = 0.3$. There is a convergence with increasing n of the simulation data at long times to the Enskog nonsingular function given in Eq. (31) (see also the upper graph of Fig. 7

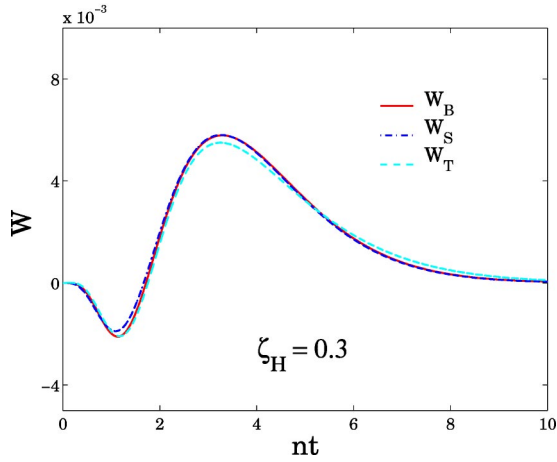


FIG. 12. A comparison between $W_{B,\infty}(t)$, $W_{S,\infty}(t)$, and $W_{T,\infty}(t)$ for the packing fraction $\zeta_H=0.3$.

for the comparable shear stress relaxation case). In Fig. 14 we show the parameter a_n versus $1/n$, estimated using the D approach for various packing fractions. Again we see that a_n appears to converge to $\sqrt{2}$ as for the bulk and shear time correlation functions. Figure 15 shows the decomposition of C_T into the same components as for C_S given in Fig. 11. The behavior is much the same. The heat flux time correlation functions $C_T(t)$ can also be fitted to the general scheme of Eq. (50), and we again find that with X_3 , $A=1.5$ is the optimum case, although the agreement is not as good. It can be seen in Fig. 12 that $w_{T,\infty} \approx w_{B,\infty}$.

V. CONCLUSIONS

Dufty made a formal analysis of the shear stress autocorrelation function in the transition region between the steeply repulsive soft sphere fluid and the hard sphere fluid [3]. This function, Dufty showed, consists in the hard sphere limit of a singular part, with the singularity at time $t=0$, and a nons-

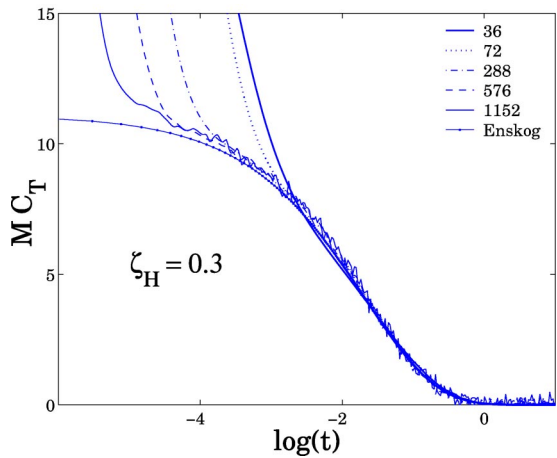


FIG. 13. The unnormalized heat flux time correlation function $C_T(t)$ vs $\log(t)$ for various n values at the packing fraction $\zeta_H = 0.3$. The approach towards the Enskog function with increasing n is clearly visible (see also the top graph of Fig. 7). M in the figure stands for M_∞ .

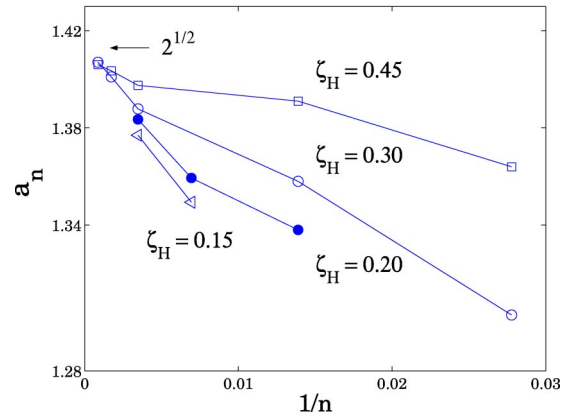


FIG. 14. The parameter a_n vs $1/n$ estimated from the D fitting approach for C_T . The solid lines drawn through the data for each packing fraction are to guide the eye. The X_3 function with $A = 1.5$ was applied.

ingular part. The former dominates at short times, $t \rightarrow 0$, and the latter tends to the Enskog solution, and is the main part, at long (mean collision) times. Dufty represented the singular part as $\text{sech}(a_n n t)$, where a_n is a disposable parameter and n is the exponent or stiffness parameter in the soft sphere potential. A time-dependent X function was introduced to weight the analytic functions for these two extremes at all times but especially in the crossover period between where the singular and nonsingular terms each dominate. This crossover period is centered around approximately the duration of a binary “collision.”

This approach has been extended here. We have considered the time correlation functions used in the Green-Kubo formulas for the bulk viscosity and thermal conductivity. The bulk viscosity is expressed in terms of the pressure time correlation function, which is entirely singular in the hard sphere limit, and therefore provides a useful prototype case to explore the singularity at $t=0$.

Many of the simulations were carried out densities where the Enskog theory gives an accurate result for the transport

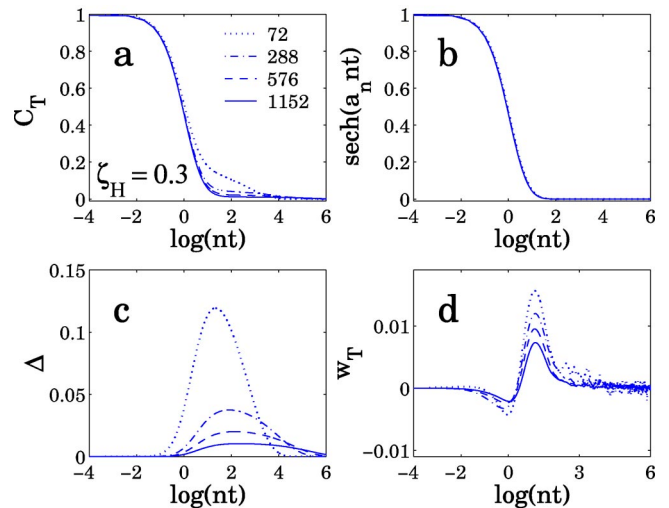


FIG. 15. As for Fig. 11, except the heat flux correlation function $C_T(t)$ is analyzed.

coefficient. The sech function used by Dufty to represent the singularity is unable to reproduce the Enskog bulk viscosity and produce the correct short-time decay behavior for any given value of a_n . The first condition is met if $a_n = \pi^{3/2}/4$, but this value does not satisfy the second condition. A combination of the sech and a perturbation function $w(t)$ is sufficiently versatile to satisfy these two requirements. This function has the limit that $w(t) \rightarrow 0$ for $t \rightarrow 0$ and $t \rightarrow \infty$. We compared various procedures to obtain the optimum value of a_n in this more general formulation. In the most satisfactory approach, we show that the simulation data are consistent with $a_n \rightarrow \sqrt{2}$ in the hard sphere ($n \rightarrow \infty$ limit), which is the result necessary to have the correct initial decay of the pressure correlation function. This limit appears to be independent of density. A possible analytic form for $w(t)$ is suggested which fits the simulation derived correlation functions very well for the steep soft potentials and in the hard sphere limit, and satisfies a number of self-consistency requirements.

We performed a similar analysis of the shear stress and heat flux correlation functions. We show that the $w(t)$ function appears to be the same as the bulk case in the hard sphere limit. We also suggest an improved analytic form for the $X(t)$ crossover function in these two cases.

The treatment presented here has been for spheres. One might ask if it can be adapted for two dimensions (2D)? In 2D, the issue of transport is still an equivocal subject because of the predicted existence of long time $\sim t^{-1}$ tails in the velocity and purely kinetic part of the time correlation functions for collective properties. Therefore, in 2D the integral

over such a tail in the velocity autocorrelation function, and hence the self-diffusion coefficient, cannot exist (at least in the thermodynamic limit) [20,21]. On the basis of the same conjecture, as the long-time behavior of the complete shear stress or heat flux autocorrelation function does not differ qualitatively from the kinetic part, the same conclusion might be reached for viscosity and thermal conductivity. Thus hydrodynamics in the conventional sense does not exist in 2D. The situation is still far from clear, however, with a shear viscosity actually being measurable in 2D nonequilibrium MD studies at finite shear rate [22,23] (see also Ref. [24] for a corresponding 3D simulation). Therefore we are reluctant to make any definitive statements about the feasibility of extending the present treatment to 2D. We cannot even be sure that the sech function will play the same role in 2D as in 3D, for example.

ACKNOWLEDGMENTS

A.C.B. and D.M.H. acknowledge the Royal Society (London) and the Polish Academy of Sciences for funding this collaboration. The work was partially supported by the Polish Committee for Scientific Research (KBN) Grant No. 4T11F01023. D.M.H. acknowledges the Engineering and Physical Sciences Research Council of Great Britain (EPSRC) for funding workstations used to carry out the computational aspects of this work. We thank Professor J. G. Powles, Physics, University of Kent, UK for kindly reading and commenting on the manuscript.

-
- [1] N.F. Carnahan and K.E. Starling, *J. Chem. Phys.* **51**, 635 (1969).
 - [2] J.-P. Hansen and I.R. McDonald, *Theory of Simple Liquids*, 2nd ed. (Academic Press, London, 1986).
 - [3] J.W. Dufty, *Mol. Phys.* **100**, 2331 (2002).
 - [4] B.J. Alder, D.M. Gass, and T.E. Wainwright, *J. Chem. Phys.* **53**, 3813 (1970).
 - [5] J.J. Erpenbeck, *Phys. Rev. E* **51**, 4296 (1995).
 - [6] S. Hess, M. Kroger, and D.J. Evans, *Phys. Rev. E* **67**, 042201 (2003).
 - [7] D.M. Heyes and J.G. Powles, *Mol. Phys.* **95**, 259 (1998).
 - [8] J.G. Powles, G. Rickayzen, and D.M. Heyes, *Proc. R. Soc. London, Ser. A* **455**, 3725 (1999).
 - [9] J.G. Powles and D.M. Heyes, *Mol. Phys.* **98**, 917 (2000).
 - [10] D.M. Heyes and J.G. Powles, *Mol. Phys.* **99**, 1077 (2001).
 - [11] D.M. Heyes, J.G. Powles, and G. Rickayzen, *Mol. Phys.* **100**, 595 (2002).
 - [12] J.C. Maxwell, *Philos. Trans. R. Soc. London* **157**, 49 (1867).
 - [13] R.W. Zwanzig and R.D. Mountain, *J. Chem. Phys.* **43**, 4464 (1965).
 - [14] D. Chandler, J.D. Weeks, and H.C. Andersen, *Science* **220**, 787 (1983).
 - [15] J.A. Barker and D. Henderson, *J. Chem. Phys.* **47**, 4714 (1967); *Rev. Mod. Phys.* **48**, 587 (1976).
 - [16] P. Résibois and M. de Leener, *Classical Kinetic Theory of Fluids* (Wiley, New York, 1977), p. 168.
 - [17] H. Sigurgeirsson and D.M. Heyes, *Mol. Phys.* **101**, 469 (2003).
 - [18] W.G. Hoover, S.G. Gray, and K.W. Johnson, *J. Chem. Phys.* **55**, 1128 (1971).
 - [19] J.-P. Boon and S. Yip, *Molecular Hydrodynamics* (McGraw-Hill, New York, 1980).
 - [20] M.H. Ernst, E.H. Hauge, and J.M.J. van Leeuwen, *Phys. Rev. Lett.* **25**, 1254 (1970).
 - [21] J.R. Dorfman and E.G.D. Cohen, *Phys. Rev. Lett.* **25**, 1257 (1970).
 - [22] D. Gravina, G. Ciccotti, and B.L. Holian, *Phys. Rev. E* **52**, 6123 (1995).
 - [23] W.G. Hoover and H.A. Posch, *Phys. Rev. E* **51**, 273 (1995).
 - [24] M. Ferrario, G. Ciccotti, B.L. Holian, and J.P. Ryckaert, *Phys. Rev. A* **44**, 6936 (1991).